Physical Review

JAN 25 1968

Spin-Lattice Interaction in Ruby Measured by ESR in Uniaxially Stressed Crystals*

R. B. Hemphill≠, P. L. Donoho, and E. D. McDonald≠

William Marsh Rice University, Houston, Texas

Abstract

The spin-lattice Hamiltonian first proposed by Van Vleck to explain electronic spin-lattice relaxation has been experimentally determined for Cr^{3+} ions in ruby single crystals. Its magnitude was obtained through measurements on the effect of applied uniaxial stress on the ESR spectrum of the Cr^{3+} ions. The spin-lattice Hamiltonian was found to be a quadratic spin operator, in agreement with Van Vleck's prediction, with no evidence for any other spin dependence. It was also determined through these measurements that the Cr^{3+} ions can be considered, for interactions with lattice modes, to occupy two inequivalent types of site in the Al_2O_3 lattice.

* Supported by National Aeronautics Space Administration

≠ Now at Texas Instruments, Inc., Dallas, Texas

≠ Now at Texaco, Inc., Houston, Texas

I. Introduction

The spin-lattice interaction for an insulating paramagnetic crystal was first treated successfully by Van Vleck[1] in terms of an interaction Hamiltonian derived from crystal-field theory. In Van Vleck's treatment the interaction between the magnetic moment of an ion and vibrations of the crystal lattice comes about indirectly: the lattice vibrations modulate the crystal field, thereby perturbing the orbital state of the ion; spin-orbit coupling then transmits this perturbation of the orbital electronic motion to the spin of the ion. Because this interaction between the lattice vibrations and the spin of the ion is a second-order process, Van Vleck found for the iron-group ions that he considered, which have strongly quenched orbital angular momentum, that the dominant part of the interaction can be expressed as an operator quadratic in the effective spin of the ion. This spin operator, the spin-lattice Hamiltonian, is also, to first order, linearly dependent on the lattice strain, and it therefore leads to the one-phonon spin-lattice relaxation which dominates relaxation processes at low temperature.

Using microwave-ultrasonic techniques Shiren and Tucker[2] verified Van Vleck's prediction of the quadratic spin dependence of the spin-lattice Hamiltonian, and they determined the magnitude of the interaction for several iron-group ions[3,4]. It was shown by Shiren[5] and by Donoho[6] that one-phonon relaxation times predicted from experimentally measured values of Van Vleck's spin-lattice Hamiltonian are in good agreement with observed relaxation times.

An excellent review of experimental and theoretical work on spin-lattice interactions for iron-group ions has recently been published by Tucker[7].

This paper describes a measurement of the spin-lattice Hamiltonian for Cr^{3+} ions in ruby. In this experiment uniaxial stress was applied to single crystals of ruby along various crystallographic directions, and the resulting changes in the ESR spectrum were measured accurately at a frequency of approximately 10.0 GHz. These changes are interpreted as being due to a spin-lattice Hamiltonian quadratic in spin and linear in the lattice strain due to the applied stress. This stress-induced spin-lattice Hamiltonian is regarded as a perturbation added to the normal spin Hamiltonian of the Cr^{3+} ion; this perturbation causes a shift in the energy levels of the ion. From the measurements described here, most of the quantities characterizing the spin-lattice Hamiltonian were determined to an accuracy of several per cent. In addition it was determined that no additional terms in the spin-lattice Hamiltonian, such as terms linear in the spin, are present to any appreciable extent. It was further determined that the Cr^{3+} ions in ruby occupy two inequivalent sites with respect to their interaction with lattice strain, resulting in different values for the spin-lattice Hamiltonian constants for the two sites. This result is similar to that obtained by Royce and Bloembergen[8] in studying the effect of an applied electric field on the ESR spectrum of ruby. Measurements similar to those reported here have been carried out by Feher and Watkins[9] and by Feher[10] for several iron-group ions in MgO.

The results reported here are in good agreement with ultrasonic-paramagnetic-resonance measurements of Tucker[4], and Dobrov[11].

II. Theory

In order to facilitate understanding of the experimental method used here and the analysis of the results, certain aspects of the theory of spin-lattice interactions and its application to the experimental situation studied here must be considered. Only a rather phenomenological treatment is undertaken, however, since a detailed derivation of the spin-lattice Hamiltonian has been given by Van Vleck[1] and, more recently, by Mattuck and Strandberg[12].

The Cr^{3+} ion in ruby is in a trigonal environment which leads to an axially symmetric spin Hamiltonian

$$H_s = g_{\parallel}\beta H_z S_z + g_{\perp}\beta(H_x S_x + H_y S_y) + D(S_z^2 - 5/4) \qquad (1)$$

where the g-tensor is nearly equal to that for a free electron because of the strong orbital quenching. The effect of a crystal-field component of symmetry lower than trigonal would be to introduce additional quadratic spin terms, but such a field would have only a very small effect on the value of the g-tensor. This fact is clearly exhibited in a comparison of the spin Hamiltonian of the Cr^{3+} ion in ruby with that in MgO. The large trigonal field introduces a zero-field splitting, 2D, in the case of ruby, but the g-tensors in the two cases are only slightly different. Consequently, when the lattice is strained, resulting in the production of crystal-field components of lower symmetry than in the unstrained crystal, it can

reasonably be expected that the strain-induced perturbation to the spin Hamiltonian would be predominantly quadratic in the spin. Although a term linear in both spin and magnetic-field strength might also be present, it should be quite small in its effect compared to the quadratic term. Mattuck and Strandberg[12] have, in fact, shown that the ratio of the term linear in spin to the quadratic term is approximately the ratio of the Zeeman energy to the spin-orbit energy. The linear term in this case should, therefore, be roughly two orders of magnitude smaller than the quadratic term, and it is not considered further in this discussion.

The most general quadratic, Hermitian spin operator which can be used for the perturbing spin-lattice Hamiltonian is

$$H_{SL} = \sum_{ij} F_{ij} S_i S_j \qquad (2)$$

where $\underset{\sim}{F}$ is a second-rank, symmetric, traceless tensor which depends on the lattice strain. For a linear strain dependence, $\underset{\sim}{F}$ can be represented in the following way:

$$F_{ij} = \sum_{kl} G_{ijkl} e_{kl} \qquad (3)$$

In the above expression, $\underset{\sim}{e}$ is the conventional strain tensor, and $\underset{\sim}{G}$ is a fourth-rank tensor symmetric to the interchange of i and j or k and l, but not necessarily symmetric to the interchange of any other pairs of indices. Because of this symmetry it is possible to use the familiar six-dimensional Voigt notation, in which the number of indices is contracted in a manner widely used in the study of the elastic properties of solids. In this notation, $\underset{\sim}{F}$ becomes a six-

dimensional vector, and $\underset{\sim}{G}$ becomes a second-rank six-dimensional tensor. It should be noted that the contracted form of $\underset{\sim}{G}$ does not necessarily possess the symmetry of elastic-constant tensors which would require that $G_{ij} = G_{ji}$.

Since the symmetry at each Cr^{3+} is C_3, the number of independent components of G is reduced from 36 to 10, and the tensor can be written in the following way:

$$G = \begin{pmatrix} G_{11} & G_{12} & -G_{33}/2 & G_{14} & -G_{25} & G_{16} \\ G_{12} & G_{11} & -G_{33}/2 & -G_{14} & G_{25} & -G_{16} \\ -(G_{11}+G_{12}) & -(G_{11}+G_{12}) & G_{33} & 0 & 0 & 0 \\ G_{41} & -G_{41} & 0 & G_{44} & G_{45} & G_{52} \\ -G_{52} & G_{52} & 0 & -G_{45} & G_{44} & G_{41} \\ -G_{16} & G_{16} & 0 & G_{25} & G_{14} & (G_{11}-G_{12})/2 \end{pmatrix} \tag{4}$$

Although the point-group symmetry at the Cr^{3+} site is only C_3, the maximum point-group symmetry of the Al_2O_3 crystal lattice is D_{3d}. If the symmetry operations of D_{3d} not included in C_3 are applied to $\underset{\sim}{G}$, it is found that all components of (4) are unchanged, except for G_{25}, G_{52}, G_{16}, and G_{45}, which merely change sign under any of the two-fold rotations of D_{3d}. Such a rotation will change $\underset{\sim}{G}$ for each ion in the manner described above, but will have no

effect on the spin Hamiltonian. Thus, the Cr^{3+} ions can be regarded as occupying two non-equivalent types of site, each of which leads to the same spin Hamiltonian, but to different spin-lattice Hamiltonians. As a result, although all ions exhibit the same ESR spectra in an unstrained crystal, ions in the different types of site will, in general, exhibit different spectra in a strained crystal. The ESR spectrum for such a strained crystal can, therefore, be expected to consist of a number of split lines. This splitting is observed experimentally in the work reported here, and its presence actually simplifies the analysis of the data, rather than introducing any complication.

Experimentally it is desired to perform measurements which permit the deduction of the components of $\underset{\sim}{G}$. This can be accomplished by measuring the magnetic-field shifts of the observable ESR absorption lines as functions of applied uniaxial stress. Extraction of the values of the components of $\underset{\sim}{G}$ is, however, somewhat complicated in this case by the fact that there are ten independent components of $\underset{\sim}{G}$ for Cr^{3+} ions in ruby and by the fact that the application of uniaxial stress generally produces an effect on the ESR spectrum dependent on several of these components simultaneously. It is necessary, therefore, to perform measurements on a number of different crystals stressed along carefully chosen directions such that a sufficient number of independent relations between the observed line shifts and splittings and the components of $\underset{\sim}{G}$ can be obtained. It is necessary, therefore, to consider the choice of appropriate crystallographic directions for the application of uniaxial in order

to clarify the experimental technique and the analysis of the data to be described in the following sections.

If the total spin Hamiltonian, the sum of equations (1) and (2), is diagonalized under the assumption that the components of $\underset{\sim}{F}$ are small compared to both the Zeeman energy and the zero-field splitting energy, 2D, a linear relationship between the shift or splitting of any resonance line and the components of $\underset{\sim}{F}$ can be derived. Combination of this relationship with equation (3) then gives the dependence of the line shift or splitting on the components of $\underset{\sim}{G}$ and on the strain resulting from the applied uniaxial stress. The diagonalization of the spin Hamiltonian is first considered.

The secular equation for the eigenvalues of the spin Hamiltonian is a quartic equation in the energy whose solution provides four allowed values of the energy, E_i. Because of the zero-field splitting, all six of the possible transitions between these levels are generally allowed, resulting in six observable resonance lines. The transition between levels $\underline{i}$ and $\underline{j}$ will be designated the $\underline{ij}$ transition, with corresponding transition frequency $\nu_{ij} = (E_i - E_j)/h$. The value of the magnetic-field strength at resonance will be designated H_{ij}. The value of the resonance field for a particular transition is a function of the angle between the field and the c-axis of the crystal. Experimentally, the resonance lines are observed at a fixed transition frequency by varying the magnetic-field strength through the resonance value, so that the effect of applied uniaxial stress, which varies the energy levels, is most conveniently described in terms of the shift in the resonant magnetic-field strength when stress is

applied. If the stress-dependent line shift is denoted, for the ij transition, by ΔH_{ij}, then the shift at constant transition frequency ν_{ij} can be expressed as

$$\Delta H_{ij} = \Sigma_k (\partial H_{ij}/\partial F_k) F_k \qquad (5)$$

where the partial derivatives of the resonance field, H_{ij}, with respect to the components of $\underset{\sim}{F}$ are evaluated at constant ν_{ij} from the implicit solution of the secular equation for the resonance field. If the x-z plane is chosen as the plane containing the c-axis of the crystal and the magnetic field, then it is found that $\partial H_{ij}/\partial F_k$ is zero unless k = 1, 2, 3, or 5. These derivatives are functions of the angle between the c-axis and the magnetic field, and are plotted in figures 1 and 2 for the more important transitions observed in this experiment. In these figures and in all subsequent discussion, the energy levels are numbered from 1 to 4 in order of decreasing energy. The derivative $\partial H_{ij}/\partial F_2$ is not plotted, since it is just the negative of $\partial H_{ij}/\partial F_1$.

The dependence of ΔH_{ij} on the components of $\underset{\sim}{G}$ can now be calculated if the dependence of the components of $\underset{\sim}{F}$ on the components of $\underset{\sim}{G}$ and on the strain can be evaluated. As explained in Section III, it was necessary experimentally to measure the component of the strain along the axis of uniaxial stress rather than to measure the stress itself. It is, therefore, most convenient to express the dependence of $\underset{\sim}{F}$ on $\underset{\sim}{G}$ in terms of this measured strain. In the diagonalization of the spin Hamiltonian and the computation of the derivatives, $\partial H_{ij}/\partial F_k$, it is most convenient to use the coordinate

system already described, in which the z-axis is the c-axis of the crystal and the magnetic field lies in the x-z plane at an angle θ to the z-axis. Consequently, in equation (5) the components of $\underset{\sim}{F}$ are also evaluated in this coordinate system. However, as explained in what follows, the crystal may be rotated so that its a-axis lies at any angle to the x-z plane. It is most useful to express the components of $\underset{\sim}{G}$ in some coordinate system fixed in the crystal, preferably the same coordinate system normally used for the evaluation of the elastic constants. In the following considerations, therefore, both the elastic compliance and $\underset{\sim}{G}$ are evaluated in a coordinate system whose x-axis is the crystallographic +a-axis and whose z-axis is the c-axis. With reference now to the original coordinate system used in the diagonalization of the spin Hamiltonian, let the crystal be oriented with its +a-axis at an angle $-\Phi$ to the x-axis. Let the uniaxial stress be applied in the x-z plane at an angle Θ to the z-axis. Then, if the elastic compliance is $\underset{\sim}{s}$, and the component of the strain along the stress axis is e, the components of $\underset{\sim}{F}$ can be written as follows:

$$\begin{aligned}(F_1-F_2)/e = {} & (G_{11}-G_{12})[(s_{11}-s_{12})\sin^2\Theta - s_{14}\sin 2\Theta \sin 3\Phi]/s' \\ & + G_{14}[2s_{14}\sin^2\Theta - s_{44}\sin 2\Theta \sin 3\Phi]/s' \\ & + (G_{25}-0.070G_{16})(s_{44}\sin 2\Theta \cos 3\Phi)/s'\end{aligned} \tag{6}$$

$$\begin{aligned}F_3/e = {} & G_{33}(s_{13}\sin^2\Theta + s_{33}\cos^2\Theta)/s' \\ & -(G_{11}+G_{12})[(s_{11}+s_{12})\sin^2\Theta + s_{13}\cos^2\Theta]/s'\end{aligned} \tag{7}$$

$$F_5/e = G_{41}[(S_{11}-S_{12})\sin^2\Theta \sin 3\Phi - S_{14}\sin 2\Theta]/s'$$
$$+ G_{44}(S_{14}\sin^2\Theta \sin 3\Phi - S_{44}\sin 2\Theta)/s'$$
$$- (G_{52}+0.159\,G_{45})(S_{11}-S_{12})\sin^2\Theta\cos 3\Phi/s' \qquad (8)$$

In the above expressions the quantity s' is the component of the elastic compliance tensor in a coordinate system whose x-axis is the stress axis. The values for the components of the elastic compliance used in the analysis of the data in this experiment were those obtained by Wachtmann et al[13].

It can be seen from expressions (6)-(8) that if the stress is applied in the m-c plane, $\Phi = 90°$, there is no dependence of the components of $\underset{\sim}{F}$ on those components of $\underset{\sim}{G}$ which change sign between the two non-equivalent sites discussed previously. Consequently, for stress applied in the m-c plane the stress-dependent line shifts will depend only upon G_{11}, G_{12}, G_{33}, G_{14}, G_{41}, and G_{44}, and there will be no line splitting. For stress applied in any other plane, however, there will occur both line shifts and splittings, but the splittings will depend only upon G_{25}, G_{52}, G_{16}, and G_{45}. It is important to observe, however, that the components of $\underset{\sim}{G}$ which lead to line splitting occur in equations (6)-(8) only in the combinations $(G_{25}-0.070\,G_{16})$ and $(G_{52}+0.159\,G_{45})$. This fact means, of course, that measurement of the line splittings can only provide the values of these two combinations of these four components of $\underset{\sim}{G}$, and not all four individual values.

The combination of equation (5) with equations (6)-(8) provides the desired relationship between the line shifts and splittings and the components of $\underset{\sim}{G}$. Inspection of these equations shows that a sufficient number of independent relations will be obtained for the determination of all the components of $\underset{\sim}{G}$, with the exception noted above, if the line shifts are measured for three different directions of the applied stress in the m-c plane ($\Phi = 90^\circ$) and the line splittings are measured for two different directions of stress in the a-c plane ($\Phi = 0^\circ$).

III. Experimental Procedure

Experimentally it was necessary to apply stress in the horizontal plane, which was the plane containing the magnetic field, in order to avoid complication of the analysis described in the preceding section. In such a situation it is difficult to measure stress directly, as would be possible if, for example, the stress were applied in the vertical direction so that known weights could be used to produce the stress. It is possible, however, to measure the stress indirectly by measuring the component of strain along the stress direction. Actually, because of the treatment of the spin-lattice Hamiltonian in terms of the lattice strain, it is necessary to obtain the strain components in any event. The measurement of any one of these components, under the condition of uniaxial stress, permits the computation of all the other components. Therefore, the measurement of strain is actually a more direct measurement of the desired quantity than would be the measurement

of stress. Consequently, the strain along the stress axis was measured by means of strain gages cemented to the ruby crystal, and the stress could then be applied in the horizontal plane by means of a simple screw mechanism.

The experimental arrangement for the application of uniaxial stress is shown schematically in Figure 3, where the coordinates defined in the previous section are also shown, for clarity. The crystal was in the form of a rectangular rod, of square cross section. It was situated in the center of a TE_{201} rectangular cavity, whose dimensions were such that approximately 20 per cent of the rod was located inside the cavity. Attached to the crystal but outside the cavity were four strain gages, one on each side of the crystal. These strain gages were simple resistance gages (Baldwin-Lima-Hamilton Type SR-4) and were attached to the sample with Eastman 910 cement. All four gages were taken from the same production lot and were stated by the manufacturer to have the same gage factor within one per cent. Stress was applied by a screw mechanism not shown in Figure 3 in such a way that the stress axis could be adjusted slightly. This adjustment of the stress axis was found to be necessary in order to insure that the stress be truly uniaxial and uniform, with no shear components. Early measurements on ruby[14] were found to be nonreproducible to some extent because of nonuniformity of the stress and because of some bending of the crystal. It was found, for example, that unless the stress axis was very carefully adjusted the strain measured on one side of the rod could differ greatly from that measured on the other sides.

This effect was apparently due to the fact that the ends of the sample against which the screw mechanism pressed could not be made exactly parallel and flat. It was necessary, therefore, to adjust the direction of the stress axis until all four gages indicated the same strain within $\pm$ 5 x 10^{-6}. Once this alignment was accomplished, a number of measurements at strains as high as 400 x 10^{-6} could be made without requiring further realignment. The reproducibility of the results and the good agreement with theory which is discussed in the following section indicated that this method of aligning the stress axis was adequate.

The ruby crystals used in this experiment were stated by the manufacturer to be low-strain laser-quality crystals containing 0.05 per cent Cr^{3+} ions. Since the concentration of Cr^{3+} ions was not important for this experiment, no attempt was made to determine it more accurately. The samples were oriented by means of a Laue back-reflection X-ray camera to an accuracy of approximately 0.3° and were cut with a precision saw into rectangular rods of length 1.5 cm and 0.3-cm square cross section. The orientations for the five samples used were the following:

Sample No. 1: Stress along c-axis (Θ = 0°).

Sample No. 2: Stress in m-c plane at 45° to c-axis (Θ = 45°, Φ = 90°).

Sample No. 3: Stress along m-axis (Θ = 90°, Φ = 90°).

Sample No. 4: Stress in a-c plane at 45° to c-axis (Θ = 45°, Φ = 0°).

Sample No. 5: Stress along a-axis (Θ = 90°, Φ = 0°).

The first three samples were used for line-shift measurements, and the last two were used for line-splitting measurements.

The ESR measurements were made at room temperature with a conventional X-band spectrometer operating at a frequency of approximately 10.1 GHz. The magnetic-field strength at the center of each line was measured as a function of measured strain using an NMR gaussmeter. Line shifts in the range 10 to 50 oersteds were observed typically, and it was estimated that they could be measured to an accuracy of approximately 0.25 oersted. The data were recorded in the form of line shift (or splitting) from the unstrained position versus strain. Measurements were made for each observable transition at several values of the angle between the field and the c-axis. For each transition and angle the quantity $\Delta H_{ij}/e$ was obtained. Through the use of equations (5)-(8) a set of relations between this quantity and the components of $\underset{\sim}{G}$ was obtained. The components of $\underset{\sim}{G}$ could then be obtained by a straightforward least-squares analysis of the data.

IV. Results

The analysis of the data by least-squares techniques yielded the following results:

$$G_{11} = 4.57 \pm 0.3 \text{ cm}^{-1} \qquad G_{14} = -0.43 \pm 0.13 \text{ cm}^{-1}$$

$$G_{12} = -1.94 \pm 0.3 \text{ cm}^{-1} \qquad G_{41} = -0.63 \pm 0.30 \text{ cm}^{-1}$$

$$G_{33} = 6.40 \pm 0.13 \text{ cm}^{-1} \qquad G_{25} - 0.070\, G_{16} = \pm 1.50 \pm 0.2 \text{ cm}^{-1}$$

$$G_{44} = 1.97 \pm 0.15 \text{ cm}^{-1} \qquad G_{52} + 0.159\, G_{45} = \pm 1.43 \pm 0.3 \text{ cm}^{-1}$$

Curves computed from these least-squares values of the components of $\underset{\sim}{G}$ are compared in Figures 4-7 to the data. The extremely good fit, with no systematic deviations between the curves and the data points, is very good evidence that the predicted form of the spin-lattice Hamiltonian, given in equation (2), is the correct form. If there were an appreciable term in the spin-lattice Hamiltonian linear in spin, then the computed curves would show a systematic deviation from the data points.

As observed previously, it is impossible to obtain the individual values of G_{25}, G_{52}, G_{16}, and G_{45} using uniaxial stress alone. The application of some other type of stress would perhaps permit the determination of these quantities separately, but it was felt that the application of any type of stress other than the uniaxial stress employed here would be very difficult and would not yield information of great enough importance to warrant the effort.

Although there seems to be no theoretical basis for assuming a symmetry to $\underset{\sim}{G}$ of the form $G_{ij} = G_{ji}$, such a symmetry is not inconsistent with the experimental results. In fact, if the data are analyzed with the requirement of this form of symmetry, which requires that $G_{16} = G_{45} = 0$, $G_{14} = G_{41}$, $G_{25} = G_{52}$, and $G_{11}+G_{12} = G_{33}/2$, then the values obtained by the least-squares analysis are changed only slightly, and the fit of the computed curves to the experimental points is almost as good. The results, as presented here, do not exhibit this symmetry, but the degree of asymmetry is, perhaps accidentally, slight.

The value for G_{33} reported here is in agreement with the value obtained by Tucker[4], 5.7 cm^{-1}, and that obtained by Dobrov[11], 5.9 cm^{-1}, by the method of ultrasonic magnetic resonance. Dobrov's value for G_{14}, 1.55 cm^{-1}, is not, however, in agreement with the value reported here. Although Tucker's measurement of G_{33} was the first measurement of the spin-lattice Hamiltonian, the accuracy of ultrasonic measurements should not, in general, be as good as that which can be obtained by the method of uniaxial stress, because the ultrasonic measurement requires, among other things, an accurate knowledge of the resonance line shape and the ionic concentration. Ultrasonic measurements in a trigonal crystal such as ruby are particularly complicated by the large number of constants to be determined in the spin-lattice Hamiltonian.

V. Discussion

This experiment has demonstrated the validity of Van Vleck's theory of the spin-lattice interaction. In particular, the quadratic dependence of the spin-lattice Hamiltonian has been quite well demonstrated. Although the data do not permit the determination of the magnitude of any term linear in spin, it is expected that such a term should be about 100 times smaller than the quadratic term, and this magnitude is certainly too small to be detected in this experiment. It should be pointed out that the presence of a term linear in spin could best be detected by observing the effect of stress on the $+1/2 \rightarrow -1/2$ transition, where the quadratic term would have no effect. Since it is difficult to obtain a pure $+1/2 \rightarrow -1/2$

transition in ruby, an attempt was made to observe this effect in MgO. No line shift was observed, leading to the conclusion that the linear term in the spin-lattice Hamiltonian for Cr^{3+} ions is indeed negligible. A linear term does appear in the spin-lattice Hamiltonian for ions with an isolated Kramers-doublet ground state, as shown by the work of Black and Donoho[15], so that the question of whether such a term appears here is of some importance.

Preliminary values of the components of the G-tensor not differing appreciably from those reported here have been used by Donoho[6] to compute the low-temperature one-phonon relaxation times for the Cr^{3+} ion in ruby. These calculations have been found by Standley and Vaughan[16] to be in good agreement with experimental values for the relaxation times.

We have made no attempt to compute the value of the G-tensor using crystal-field theory because of the complexity of the problem. The calculation of $\underset{\sim}{G}$ in ruby should be closely related to the problem of calculating the zero-field splitting 2D, which arises from the trigonal distortion of the field from cubic symmetry and the spin-orbit coupling. A calculation of this splitting was made by Sugano and Peter[17], who found it necessary to assume substantial configuration mixing, covalency, and anisotropic spin-orbit coupling in order to obtain reasonable accuracy in their value for the zero-field splitting. More recent work by Macfarlane[18,19] has, however yielded an even better value for 2D without introducing the complications used by Sugano and Peter. In his work, Macfarlane diagonalizes the crystal field accurately for the entire d^3 configuration, and

finds that the principal contribution to 2D comes from the off-diagonal elements of the matrix, and not from the diagonal elements as assumed by Sugano and Peter. It seems quite reasonable that Macfarlane's procedure is appropriate for the computation of the G-tensor, and a calculation based on this method should yield reasonably accurate results. In fact, Sturge[20] has shown that in a uniaxial stress experiment $\Delta D/D$, which is equal to $G_{33} e/D$, is equal within experimental error to $\Delta v'/v'$, the ratio of the change in off-diagonal matrix element to the unperturbed value of the matrix element. This result seems to indicate that $\underset{\sim}{G}$ will depend strongly also on the off-diagonal components of the matrix of the perturbing field due to applied stress. It should be pointed out that Blume and Orbach[21] have computed $\underset{\sim}{G}$ for Mn^{++} ions in MgO, obtaining the correct order of magnitude, but the wrong sign for the components.

References

1. J. H. Van Vleck, Phys. Rev. 57, 426 (1940).
2. N. S. Shiren and E. B. Tucker, Phys. Rev. Letters 6, 105 (1961).
3. N. S. Shiren, Bull. Am. Phys. Soc. 7, 29 (1962).
4. E. B. Tucker, Phys. Rev. Letters 6, 183 (1962).
5. N. S. Shiren, in Magnetic and Electric Resonance and Relaxation, edited by J. Smidt (Interscience Publishers, Inc., New York, 1963).
6. P. L. Donoho, Phys. Rev. 133, A1080 (1964).
7. E. B. Tucker, Proc. IEEE 53, 1547 (1965).
8. E. B. Royce and N. Bloembergen, Phys. Rev. 131, 1912 (1963).
9. E. R. Feher and G. D. Watkins, Bull. Am. Phys. Soc. 7, 29 (1962).
10. E. R. Feher, Phys. Rev. 136, A145 (1964).
11. W. I. Dobrov, Phys. Rev. 134, A734 (1964).
12. R. D. Mattuck and M.W.P. Strandberg, Phys. Rev. 119, 1204 (1960).
13. J. B. Wachtman, Jr., W. E. Tefft, D. G. Lam, Jr., and R. P. Stinchfield, Jour. Res. Nat. Bur. Std. 64A, 213 (1960).
14. P. L. Donoho and R. B. Hemphill, Proceedings of the Eighth International Conference on Low Temperature Physics, edited by R. O. Davies (Butterworth and Co. Ltd., London, 1963) Ch. 9, 294.
15. T. D. Black and P. L. Donoho, Bull. Am. Phys. Soc. 9, 37 (1964).
16. K. J. Standley and R. A. Vaughan, Phys. Rev. 139, A1275 (1965).
17. S. Sugano and M. Peter, Phys. Rev. 122, 381 (1961).
18. R. M. Macfarlane, J. Chem. Phys. 42, 442 (1965).
19. R. M. Macfarlane, J. Chem. Phys. 39, 3118 (1963).
20. M. D. Sturge, J. Chem. Phys. 43, 1826 (1965).
21. M. Blume and R. Orbach, Phys. Rev. 127, 1587 (1962).

Figure Captions

Figure 1. Rate of change of resonance field with respect to spin-lattice interaction parameters; 12 and 23 (high field) transitions at frequency 10.1 GHz.

Figure 2. Rate of change of resonance field with respect to spin-lattice interaction parameters; 23 (low field) and 34 transitions at frequency 10.1 GHz.

Figure 3. Experimental arrangement showing orientation of ruby sample and stress axis with respect to crystallographic axes.

Figure 4. Experimental data on line shifts for Sample No. 1 ($\Theta = 0^\circ$), showing curves computed from least-squares analysis of data.

Figure 5. Experimental data on line shifts for Sample No. 2 ($\Theta = 45^\circ$, $\Phi = 90^\circ$), showing curves computed from least-squares analysis of data.

Figure 6. Experimental data on line shifts for Sample No. 3 ($\Theta = 90^\circ$, $\Phi = 90^\circ$), showing curves computed from least-squares analysis of data.

Figure 7. Experimental data on line splittings for Sample No. 4 ($\Theta = 45^\circ$, $\Phi = 0^\circ$), showing curves computed from least-squares analysis of data.

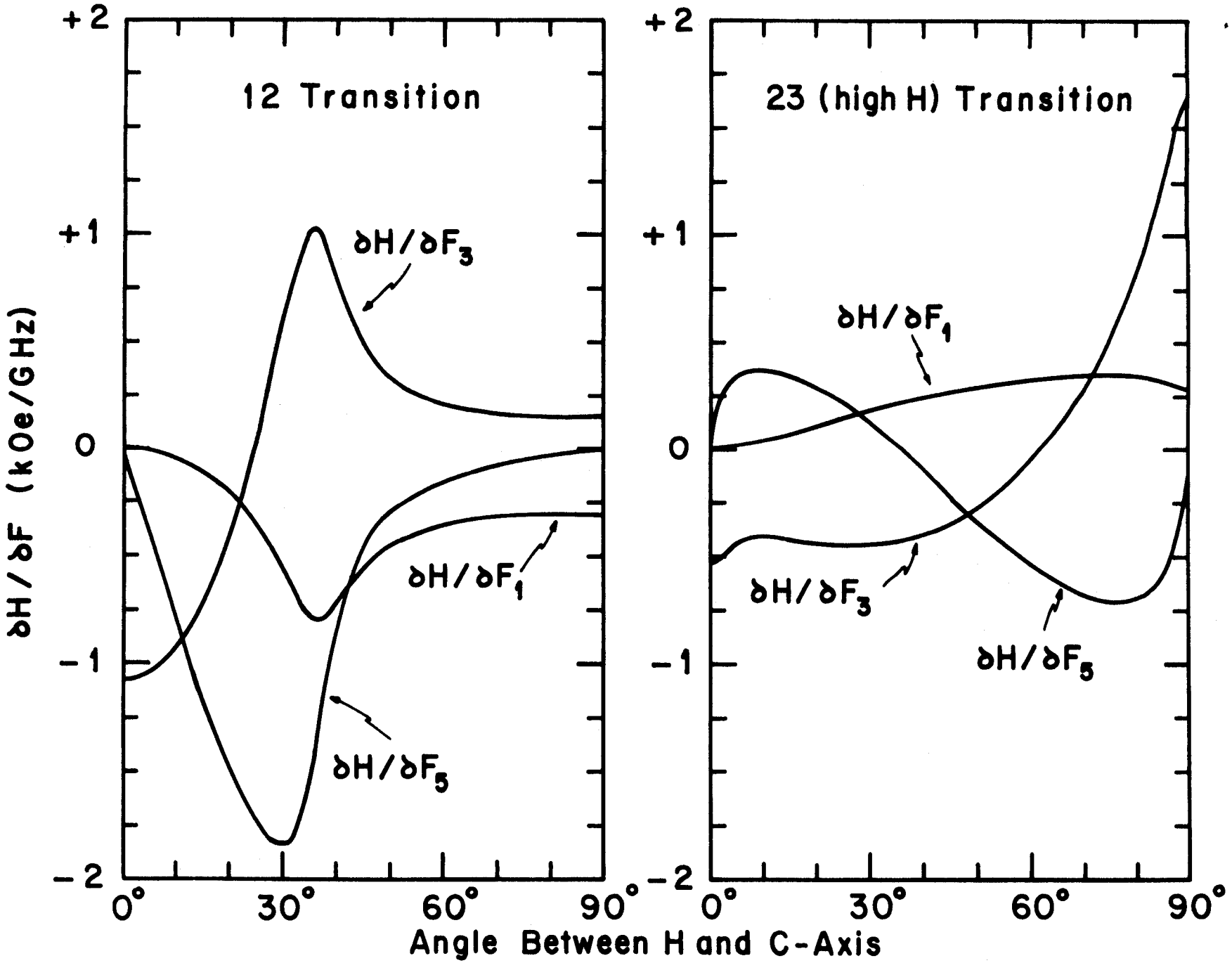
12 Transition
23 (high H) Transition
δH/δF (kOe/GHz)
+2
+1
0
-1
-2
δH/δF3
δH/δF1
δH/δF5
0°
30°
60°
90°
Angle Between H and C-Axis

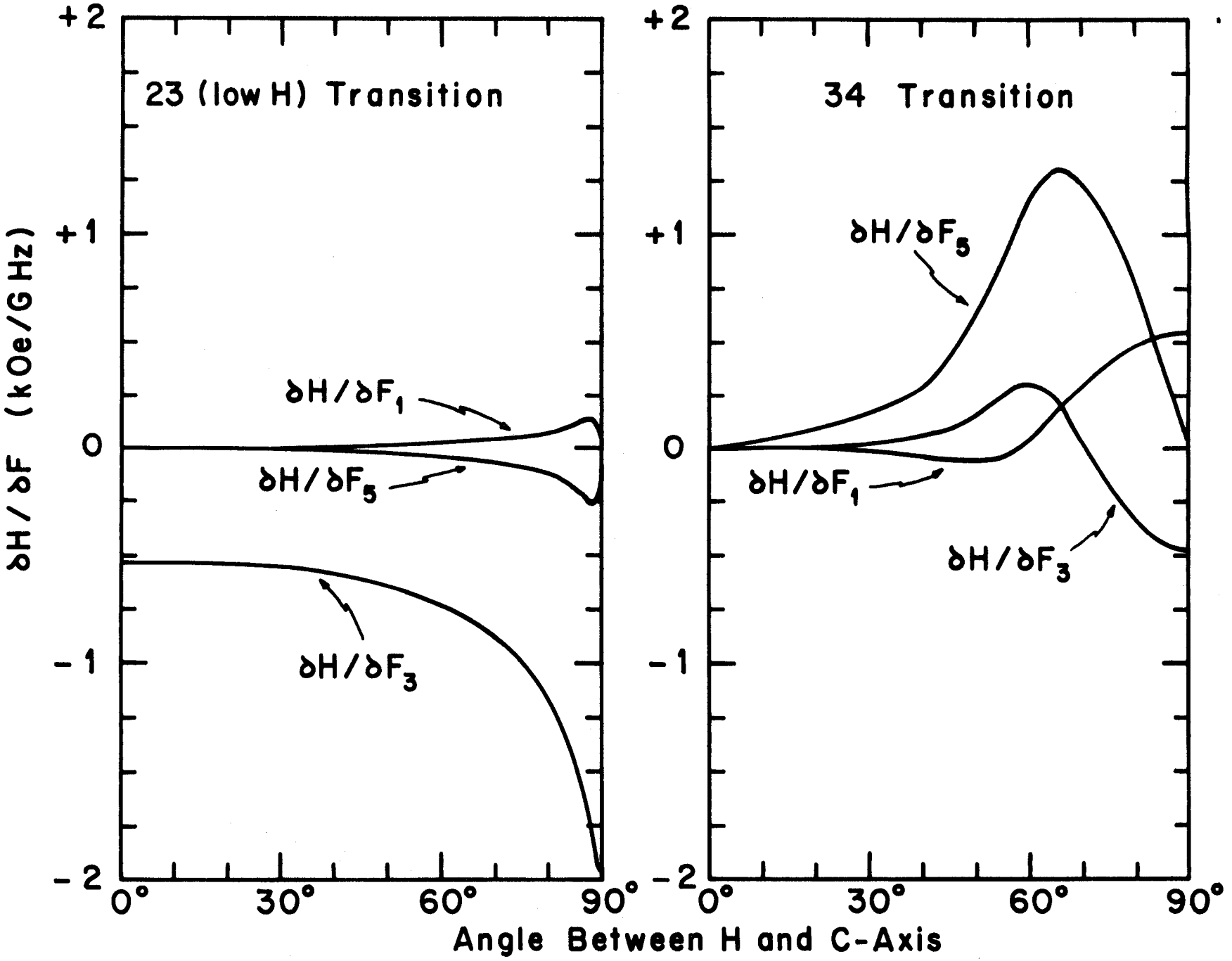
+2
+1
0
-1
-2
23 (low H) Transition
δH/δF (kOe/GHz)
δH/δF1
δH/δF5
δH/δF3
0°
30°
60°
90°
34 Transition
δH/δF5
δH/δF1
δH/δF3
Angle Between H and C-Axis

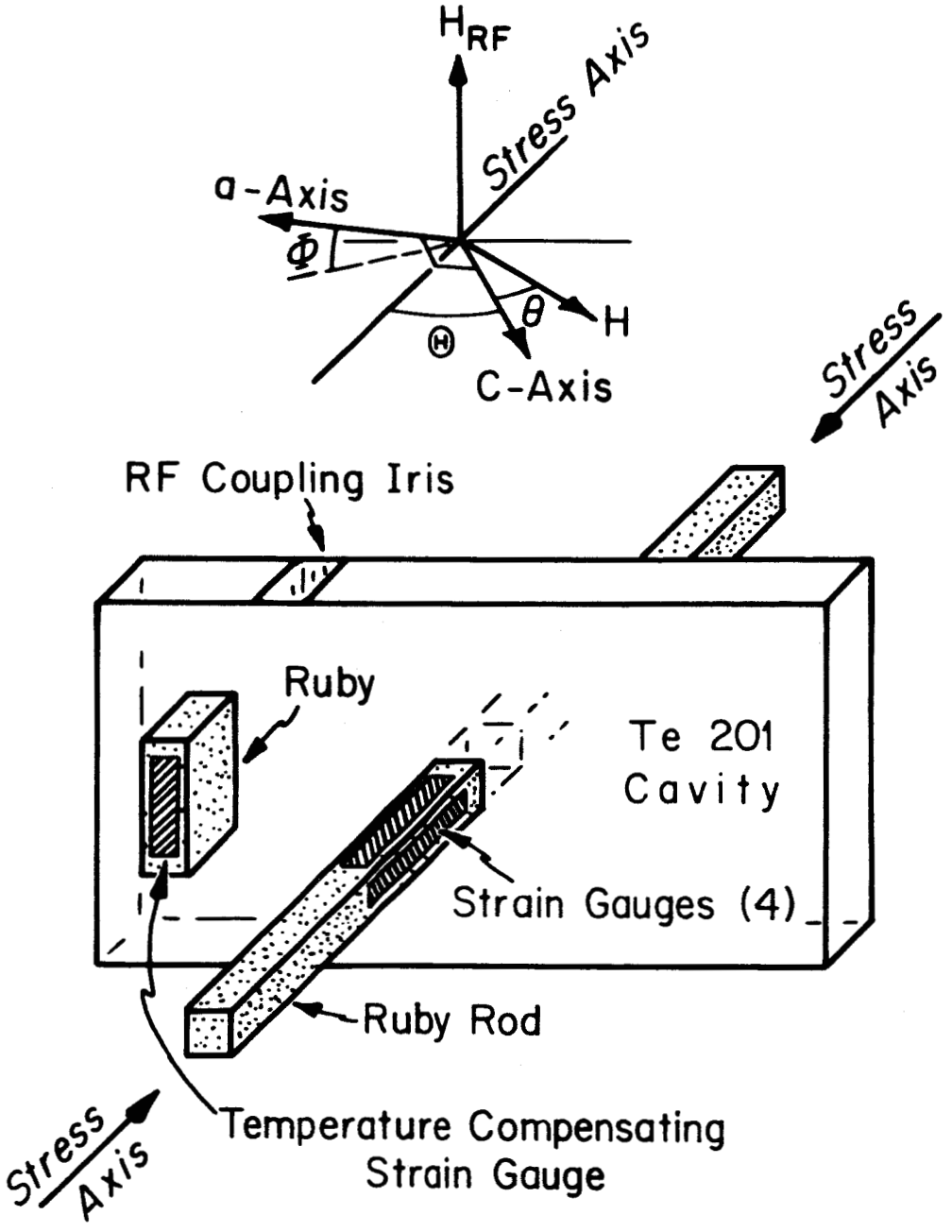
H_{RF}
Stress Axis
a-Axis
Φ
θ
H
C-Axis
Stress Axis
RF Coupling Iris
Ruby
Te 201
Cavity
Strain Gauges (4)
Ruby Rod
Stress Axis
Temperature Compensating
Strain Gauge

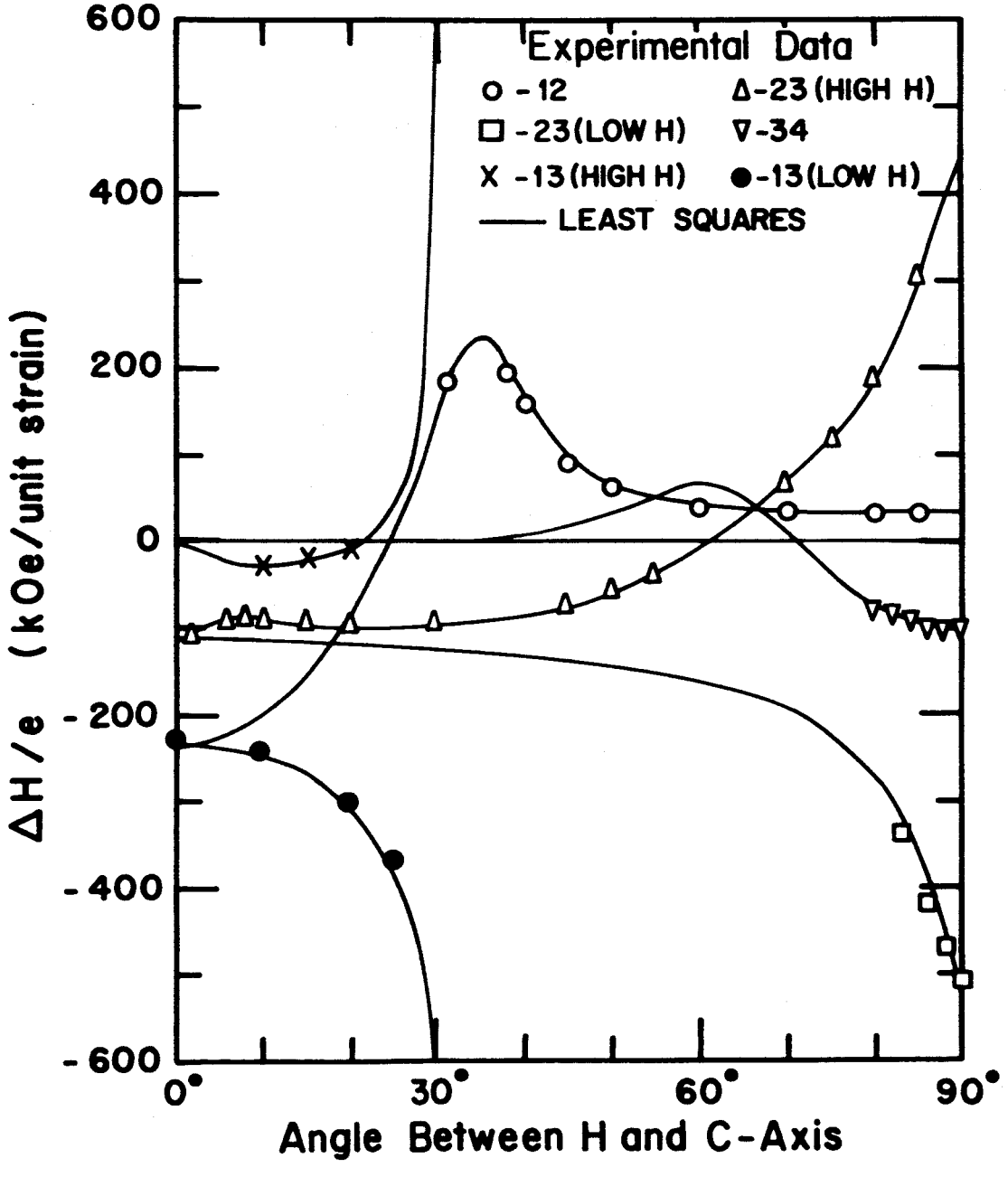
Experimental Data
o - 12
Δ-23 (HIGH H)
□ -23(LOW H)
▽-34
X -13(HIGH H)
● -13(LOW H)
—— LEAST SQUARES
600
400
200
0
-200
-400
-600
ΔH/e (kOe/unit strain)
0°
30°
60°
90°
Angle Between H and C-Axis

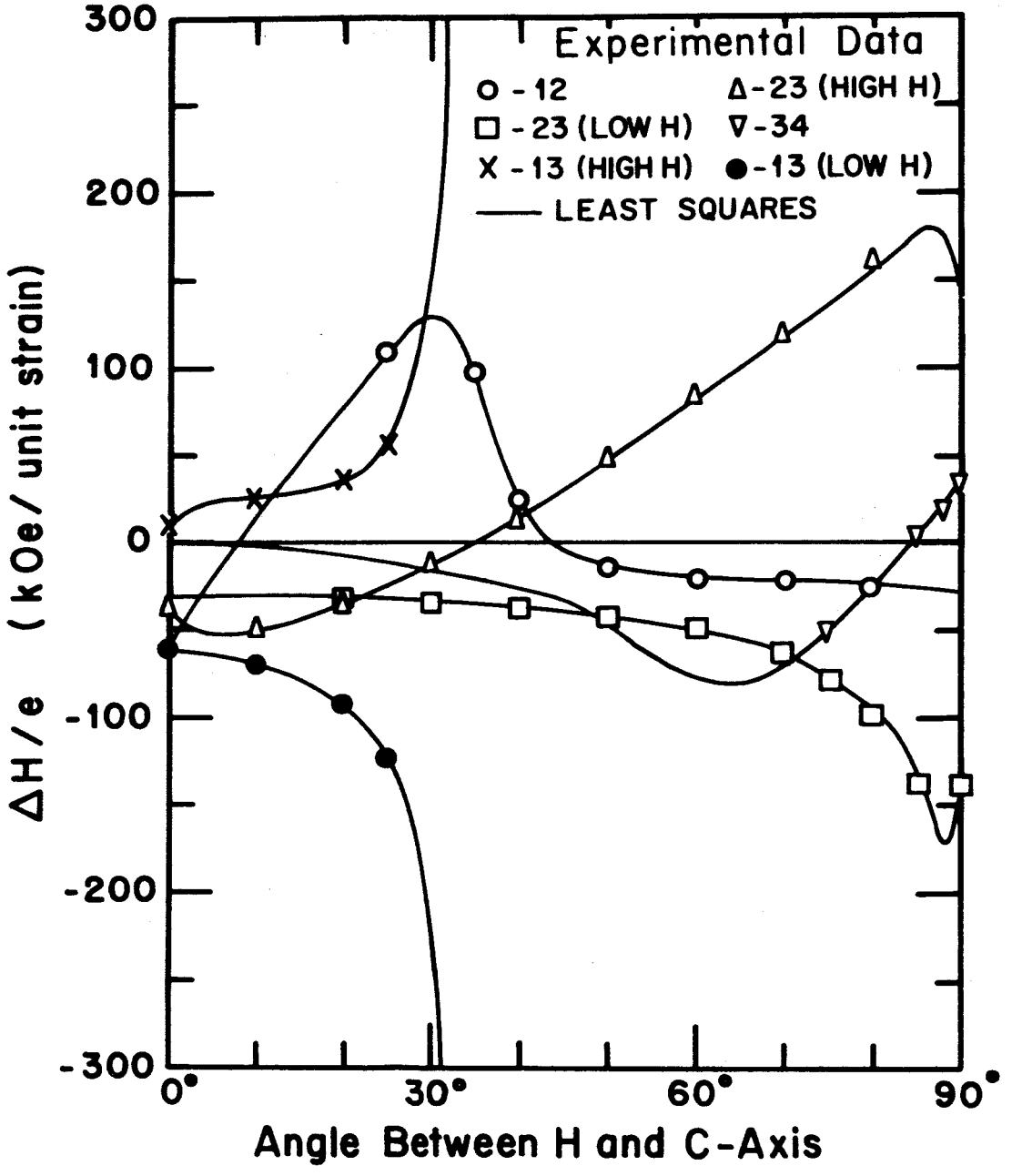
Experimental Data
O - 12
Δ - 23 (HIGH H)
□ - 23 (LOW H)
▽ - 34
X - 13 (HIGH H)
● - 13 (LOW H)
LEAST SQUARES
300
200
100
0
-100
-200
-300
ΔH/e (kOe/unit strain)
0°
30°
60°
90°
Angle Between H and C-Axis

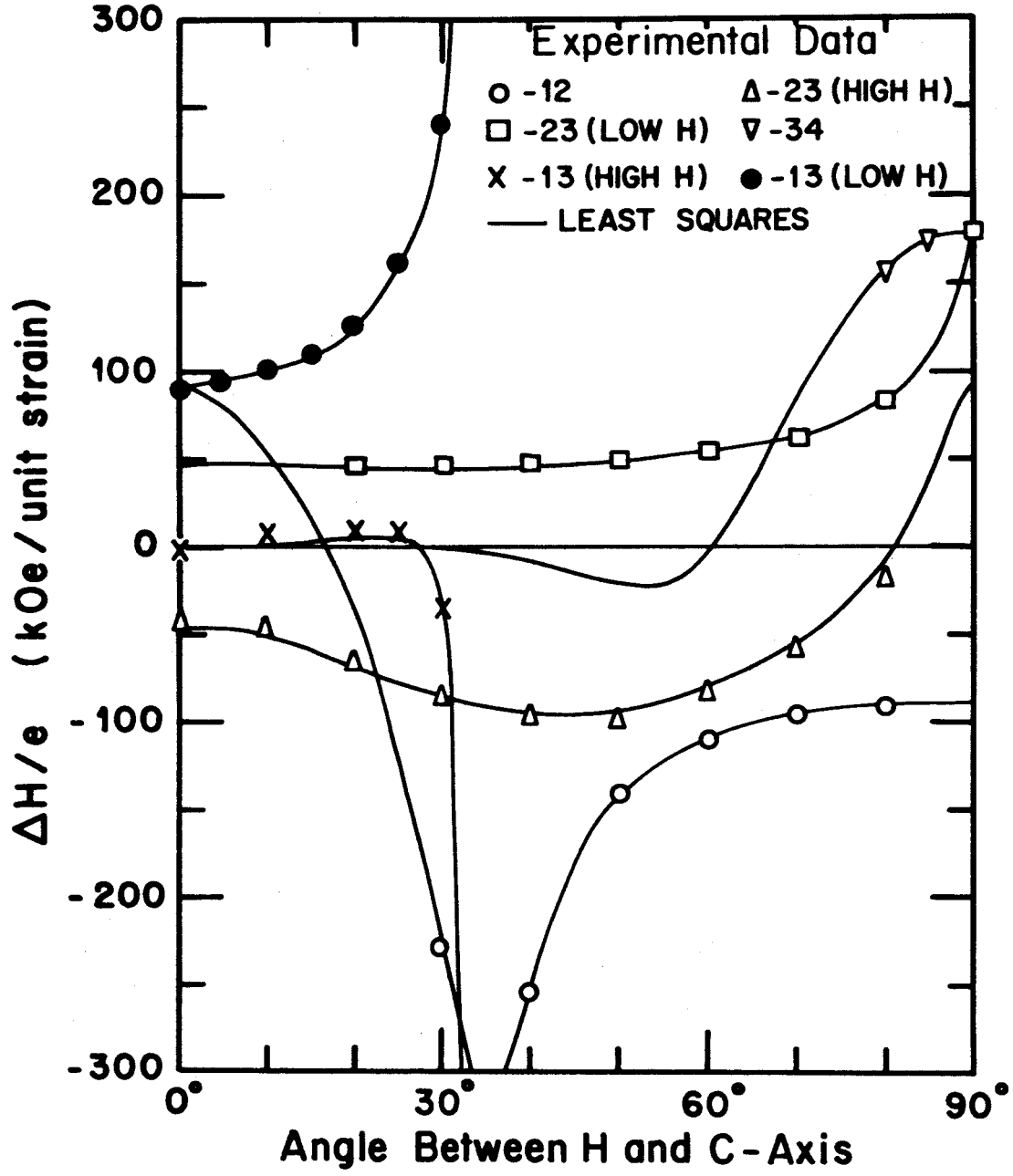
Experimental Data
o -12
Δ -23 (HIGH H)
□ -23 (LOW H)
∇ -34
X -13 (HIGH H)
● -13 (LOW H)
LEAST SQUARES
300
200
100
0
-100
-200
-300
ΔH/e (kOe/unit strain)
0°
30°
60°
90°
Angle Between H and C-Axis

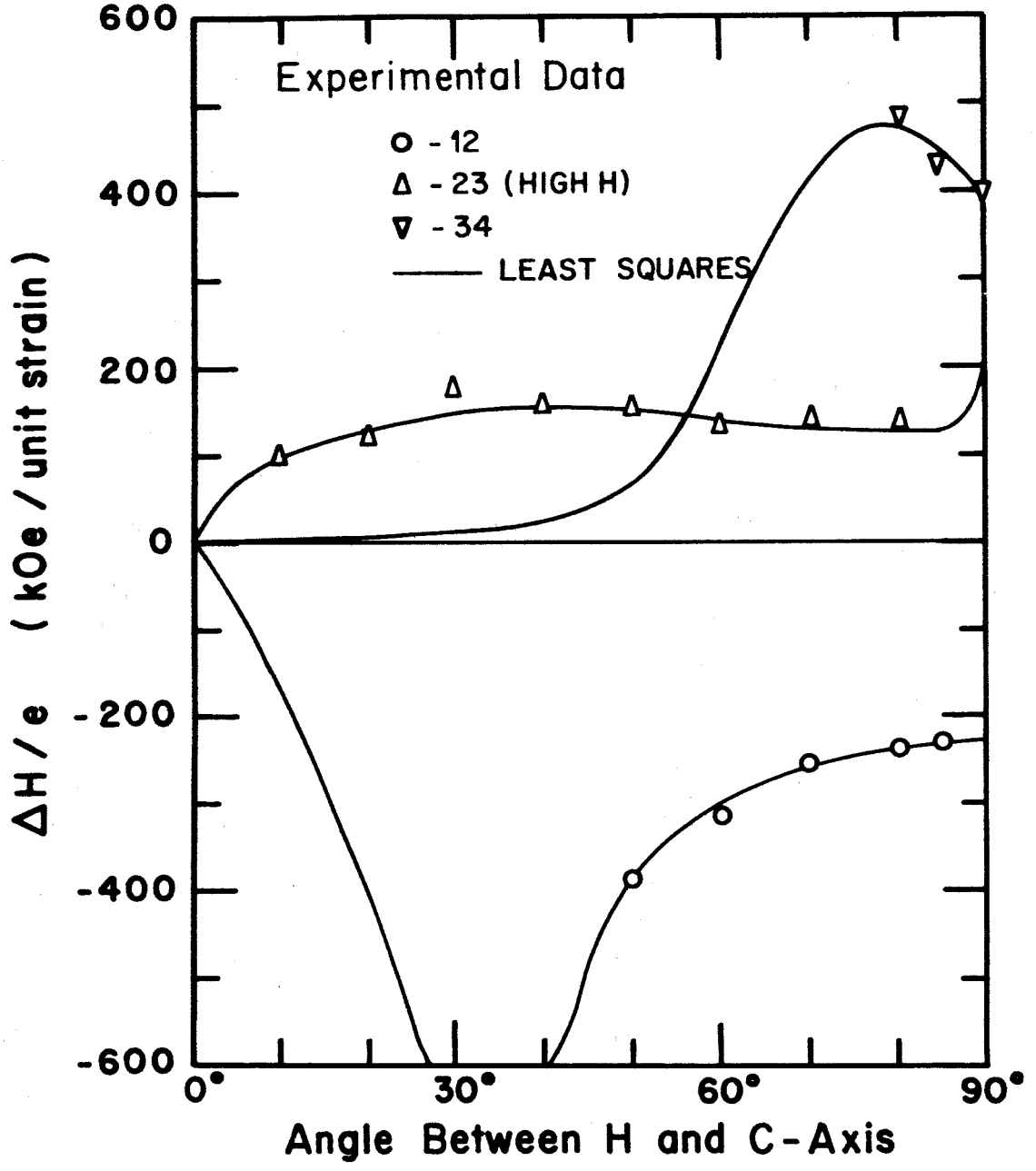
Experimental Data
o - 12
Δ - 23 (HIGH H)
▽ - 34
LEAST SQUARES
600
400
200
0
-200
-400
-600
ΔH / e (kOe / unit strain)
0°
30°
60°
90°
Angle Between H and C-Axis